Postprint of: Kozieł S., Pietrenko-Dąbrowska A., Tolerance-Aware Multi-Objective Optimization of Antennas by Means of Feature-Based Regression Surrogates, IEEE TRANSACTIONS ON ANTENNAS AND PROPAGATION Vol. 70 No 7 (2022), pp. 5636 - 5646, DOI: 10.1109/TAP.2022.3145462

Tolerance-Aware Multi-Objective Optimization of Antennas by Means of Feature-Based Regression Surrogates

Slawomir Koziel, *Fellow*, *IEEE*, and Anna Pietrenko-Dabrowska, *Senior Member*, *IEEE*

***Abstract*—Assessing the immunity of antenna design to fabrication tolerances is an important consideration, especially when the manufacturing process has not been predetermined. At the same time, the antenna parameter tuning should be oriented toward improving the performance figures pertinent to both electrical (e.g., input matching) and field properties (e.g., axial ratio bandwidth) as much as possible. Identification of available trade-offs between the robustness and nominal performance can be realized through multi-objective optimization (MO), which is an intricate and computationally expensive task. This paper proposes a novel technique for fast tolerance-aware MO of antenna structures. The key component of the presented methodology is a feature-based regression surrogate, established based on the characteristic points of antenna responses extracted from its electromagnetic (EM)-simulation data, and employed for a rapid estimation of the maximum allowed input tolerance levels for given values of performance parameters of interest. Subsequent trade-off designs are generated by tuning the antenna parameters for various assumed values of relevant figures of interest (e.g., the operating bandwidth). As demonstrated using three microstrip antennas, a rendition of performance-robustness trade-off designs can be accomplished at the cost of just about forty (for six-parameter antenna) to about eighty (for fourteen-parameter antenna) per design EM analyses of the respective structure. Reliability of the approach is validated through direct EM-driven Monte Carlo analysis at the selected designs.**

***Index Terms*— Antenna optimization; multi-objective design; fabrication tolerances; EM-driven design; surrogate modeling; response features.**

I. Introduction

Antenna manufacturing processes inherently suffer from a limited accuracy, and there is a direct relation between the achievable level of tolerances pertaining to geometry parameters and the fabrication costs. Appropriate assessment of design sensitivity to parameter deviations is therefore an important part of the antenna development process. At the same time, the best system performance—as understood traditionally (i.e., ensuring desirable levels of electrical and field parameters such as bandwidth, gain, axial ratio, etc.)—may not correspond to the maximum immunity to tolerances [1]. The robustness is also essential for devices subjected to epistemic (or systematic) uncertainties [2], e.g., varying environmental conditions (temperature, humidity), mechanical deformations (bending), or lack of precise knowledge about the material parameters (e.g., substrate permittivity). All of these may affect the system performance in an undesirable manner [3]. To ensure up-to-standard operation, sufficient safety margins are always necessary. Having in mind the aforementioned factors, including the manufacturing expenses, practically attractive designs are often sub-optimal in terms of performance, yet exhibit a sufficient level of robustness that allows for accommodating both statistical and systematic uncertainties.

From the perspective of practical design, the improvement of antenna performance is most often realized using numerical optimization methods [4]-[8]. For reliability reasons, it is normally carried out using full-wave electromagnetic (EM) simulation models. The associated computational cost is perhaps its most serious challenge, especially in the case of global search methods [9], nowadays primarily involving nature-inspired metaheuristic procedures [10]-[14]. If the fabrication tolerances are to be accounted for as well, in particular, an identification of performance-robustness trade-offs is required, the design problem becomes inherently multi-objective [15]. Multi-objective optimization (MO) is a numerically demanding process. In the case of EM-driven MO, the difficulties related to excessive computational overhead can be alleviated using surrogate modeling techniques [16], [17], where most of the operations are executed at the level of a fast replacement model (the surrogate). The latter can be either based on approximating samples EM simulation data (kriging [18], Gaussian process regression, GPR [19], support-vector machines [20], performance-driven surrogates [21], [22]) or physics-based (space mapping [23], sequential domain patching [24], Pareto-ranking-based bisection [25]). In practice, the surrogate is often iteratively refined using the high-fidelity data accumulated in the course of the optimization process [26], [27]. It is also possible to combine data-driven and physics-based surrogates to improve computational efficiency of the MO process, as suggested in [28]. Therein, kriging interpolation models rendered at the level of low-fidelity EM simulations

The manuscript was submitted on September 13, 2021. This work was supported in part by the Icelandic Centre for Research (RANNIS) Grant 2066060, and by National Science Centre of Poland Grant 2018/31/B/ST7/02369.

S. Koziel is with Engineering Optimization and Modeling Center of Reykjavik University, 102 Reykjavik, Iceland (e-mail: koziel@ru.is); A. Pietrenko-Dabrowska and also S. Koziel are with Faculty of Electronics, Telecommunications and Informatics, Gdansk University of Technology, 80-233 Gdansk, Poland.

This article has been accepted for publication in a future issue of this journal, but has not been fully edited. Content may change prior to final publication. Citation information: DOI 10.1109/TAP.2022.3145462, IEEE Transactions on Antennas and Propagation

have been corrected using space mapping and sparse high-fidelity EM data.

Accounting for tolerances requires quantification of the uncertainties [29]. For high-frequency structures, the most popular statistical performance metric is the yield [30], whereas robust design methods are concerned with yield maximization [31], [32], i.e., the increasing the likelihood of the system satisfying given performance requirements under the assumed probability distribution of the manufacturing tolerances and other relevant parameter and/or material deviations [33]. An alternative approach is seeking for the maximum level of input parameter deviations, for which the output tolerances are within acceptable limits (cf. maximum input tolerance hypervolume, MITH [34]). In any case, the estimation of statistical figures of merit is a computationally expensive task when using traditional methods. For example, direct EM-driven Monte Carlo (MC) simulation is most often prohibitive. Consequently, statistical analysis and robust design of antenna and microwave components is typically conducted with the aid of surrogate modeling methods [35]-[37]. A notable example is polynomial chaos expansion (PCE) [38], [39], which allows for evaluating statistical moments of the system outputs based on the PCE expansion coefficient, without the necessity of running MC. In [40], a technique exploiting polynomial chaos–Kriging (PC-Kriging) modeling method for fast yield estimation of multi-band antennas has been reported. The underlying concept is to replace the conventional polynomial-based trend functions by PCE, which brings additional computational savings as compared to ordinary kriging. Another option is to employ performance-driven modeling concept for cost-efficient yield optimization of antennas, as proposed in [41], where the surrogate domain is only extended towards important directions of the parameters space (those having more significant impact on the statistical figures of merit). As a result, a single surrogate constructed with a small training data set can be used, rather than a sequence of models rendered in consecutive domains relocated along the yield optimization path.

Few methods for multi-objective design of antenna structures with tolerance analysis have been reported in the literature. In [42], kriging surrogate models were used for robust MO of electromagnetic devices, with worst-case analysis conducted for Pareto-optimal designs identified using particle swarm optimization (PSO). In [34], the authors carry out multi-objective design of antenna components and antenna arrays with MITH evaluated using machine learning approach with the underlying surrogate constructed using GPR [43]. The approach proposed in [44] is perhaps the only technique where the input tolerance hypervolume is explicitly handled as one of the design objectives. Therein, three competing modeling methods are applied (polynomial regression, kriging, and GPR) to accelerate the MO process realized using the non-dominated sorting genetic algorithm (NSGA) [45]. The procedure is successfully applied to a broadband Vivaldi antenna and a capacitively-loaded monopole antenna, both described by six geometry parameters.

This paper proposes a novel surrogate-assisted procedure for rapid tolerance-aware multi-objective design of antenna components. In our approach, maximization of the input tolerances that still ensure satisfaction of the prescribed design specifications is treated as an explicit design objective. Its assessment is aided by feature-based regression surrogates constructed using characteristic points of antenna responses extracted from EM simulation data. The performance-robustness trade-off designs are generated iteratively through (local) tuning of antenna geometry parameters for different values of relevant figures of interest (e.g., the impedance bandwidth). The presented methodology is demonstrated using three microstrip antennas, including dual- and triple-band structures. The cost of the MO process is remarkably low, and corresponds to only a few dozens of EM analyses of the respective components. Reliability of the procedure is validated by means of direct EM-driven Monte Carlo analysis of the selected designs. The originality and the technical contribution of this work can be summarized as follows: (i) the development of a novel MO procedure with explicit treatment of acceptable input tolerance levels as design objective, (ii) incorporation of feature-based regression models for rapid and accurate assessment of statistical figures of merit of antenna design into the MO process, (iii) comprehensive (based on three antenna structures) demonstration of the efficacy of the presented algorithm and its low execution cost. The methodology introduced in this paper may become a useful tool for a fast rendition of alternative antenna designs representing possible trade-offs between nominal performance and immunity to manufacturing tolerances, thereby allowing the designer to select, e.g., a suitable fabrication process. Another application is to compare different designs with respect to their ability to satisfy the imposed performance requirement under the assumed parameter deviation levels.

II. Multi-Objective Antenna Parameter Tuning: Performance versus Robustness

This section provides the details of the multi-objective design procedure with tolerance analysis, proposed in the work. We start by formulating the design task (Section II.*A*), followed by uncertainty quantification approach involving response feature surrogates (Section II.*B*), as well as the outline of the iterative procedure for generating optimum trade-off designs between nominal performance of the antenna of interest and its robustness (Section II.*C*). The latter is measured by the maximum level of input tolerances, for which satisfaction of the assumed design specification is still ensured. The entire optimization framework is summarized in Section II.*D* and further explained by means of a flow diagram.

A. Problem Statement

Let $\boldsymbol{R}(\boldsymbol{x})$ denote the EM-simulated responses of the antenna at hand with $\boldsymbol{x} = [x_1 \ \ldots \ x_n]^T$ being a vector of adjustable (geometry) parameters. In specific instances, the responses of interest might be reflection $S_{11}(\boldsymbol{x},f)$, axial ratio $AR(\boldsymbol{x},f)$, or gain characteristics $G(\boldsymbol{x},f)$; in all these cases, explicit dependence on frequency f has been marked. Let F_p $(\boldsymbol{x})$ be a scalar function representing the (target) nominal performance for the antenna, i.e., assuming no fabrication tolerances or other types of

This article has been accepted for publication in a future issue of this journal, but has not been fully edited. Content may change prior to final publication. Citation information: DOI 10.1109/TAP.2022.3145462, IEEE Transactions on Antennas and Propagation

uncertainties. In this work, for the purpose of formulating and demonstrating the proposed approach, the figures of interest will be based on the target operating bandwidths.

Let us assume that f_{0k}, $k = 1, \ldots, N$, are the intended operating frequencies, and B_k be the target bandwidths over which the particular parameter $P(\boldsymbol{x},f)$ should not exceed the acceptance threshold $P_{\max}$. Given the target operating frequencies and bandwidths, the performance requirements are satisfied if

$$\max\left\{f \in \bigcup_{k=1}^{N}\left[f_{0k}-B_k, f_{0k}+B_k\right] : |P(\boldsymbol{x},f)|\right\} \le P_{\max} \quad (1)$$

Here, again, f stands for frequency. In the case of antenna input characteristics, we would have $P(\boldsymbol{x},f) = |S_{11}(\boldsymbol{x},f)|$, and, typically, the maximum acceptable level is set to be $P_{\max} = S_{11.\max} = -10$ dB. If the goal is to ensure a specific axial ratio bandwidth, we have $P(\boldsymbol{x},f) = AR(\boldsymbol{x},f)$, and the maximum acceptable level is normally set as $P_{\max} = AR_{\max} = 3$ dB.

Now, if the design problem is formulated to obtain the best possible levels of the performance parameter P over the target bandwidths, then the best nominal design (here, denoted as $\boldsymbol{x}^p$) can be obtained as

$$\boldsymbol{x}^p = \arg\min_{\boldsymbol{x}}\{\max\{f \in \bigcup_{k=1}^{N}\left[f_{0k}-B_k, f_{0k}+B_k\right] : P(\boldsymbol{x},f)\}\} \quad (2)$$

In practice, we might set $B_1(\boldsymbol{x}) = \ldots = B_N(\boldsymbol{x}) = B(\boldsymbol{x})$ (equal absolute bandwidth requirement), or $B_1(\boldsymbol{x})/f_{01} = \ldots = B_N(\boldsymbol{x})/f_{0N} = B_F(\boldsymbol{x})$ (equal fractional bandwidth requirement), and minimize $P(\boldsymbol{x},f)$ according to (2). Within this formulation, the target nominal antenna performance $F_p(\boldsymbol{x})$ will simply equal $P_{\max}$.

In the following, let $F_r(\boldsymbol{x})$ be a scalar function representing the antenna robustness, calculated using a statistical figure merit of choice. As mentioned in the introduction, this could be the fabrication yield estimated for the assumed probability distribution describing the parameter deviations, or the measure of maximum input tolerances (e.g., the tolerance hypervolume [34]) for which the performance requirements are still satisfied. In this work, it is assumed that parameter deviations follow independent Gaussian distributions of zero mean and a (common across all parameters) variance σ. In this, case, we have $F_r(\boldsymbol{x}) = \sigma(\boldsymbol{x})$, where the dependence on the design $\boldsymbol{x}$ emphasizes the fact that the maximum allowed variance is a function of antenna parameters. The assumption of joint variance for independent Gaussian distributions, is tenable, as geometry parameter deviations are determined by the fabrication process such as chemical etching. Nevertheless, this supposition can be extended to virtually any given covariance matrix describing the relationships between the design variables, e.g., due to a particular spatial allocation of the parameters. In fact, replacing joint variance (which is, in fact, an identity covariance matrix) by arbitrary covariance matrix, has no effect on the relevance and operation of the presented methodology. The only change would be the necessity of employing a different optimization routine when evaluating the function F_r in (6).

Using the notation discussed above, the tolerance-aware multi-objective antenna design task can be formulated as

$$\boldsymbol{x}^* = \arg\min_{\boldsymbol{x}}\left[F_p(\boldsymbol{x}) \quad -F_r(\boldsymbol{x})\right] \quad (3)$$

i.e., the goal is to simultaneously improve both the target nominal performance $F_p(\boldsymbol{x})$ and the robustness $F_r(\boldsymbol{x})$. Note that we put the minus sign in front of F_r in order to turn maximization of robustness into a minimization task for the sake of consistency with the treatment of F_p. Clearly, these two objectives are at least partially conflicting, in particular, imposing more demanding target nominal performance normally leads to a degradation of the robustness. Consider two specific designs, the best nominal design $\boldsymbol{x}^p$ as discussed above, and the minimum acceptable performance design, here, denoted as $\boldsymbol{x}^r$, corresponding to the highest (worst) target value of F_p that can be accepted for a given application, or any other value of the designer's choice (e.g., –10 dB in the case of reflection response, or 3 dB for the axial ratio response). Further, the design $\boldsymbol{x}^r$ is obtained to maximize F_r given the aforementioned highest values of F_p. We have

- Design $\boldsymbol{x}^p$. Because this design corresponds to be best possible performance according to the assumed requirements (e.g., the lowest in-band reflection of the antenna), it features the minimum robustness at the same time. In particular, we have zero fabrication yield, and zero levels of input tolerances ensuring the fulfilment of performance specifications. This is because any parameter deviation with respect to $\boldsymbol{x}_p$ necessarily degrades $F_p(\boldsymbol{x})$, which leads to violating the condition (1). In other words, the subset containing feasible designs with respect to the condition (1) is—assuming uniqueness of solution to (2)—a single-point set consisting of $\boldsymbol{x}^p$.
- Design $\boldsymbol{x}^r$. As this design features the largest performance margin with respect to the best nominal design $\boldsymbol{x}^p$, it exhibits the largest robustness at the same time (recall, that $\boldsymbol{x}^r$ was assumed to maximize F_r). This is because the feasible region for the highest considered value of F_p is the largest, and centering the design within it allows for maximization of the input tolerance levels, for which the performance specifications (as determined by F_p) can still be satisfied.

The set of designs which are globally non-dominated in the Pareto sense [46] with respect to the objectives F_p and F_r form the Pareto front X_P [46], representing the best possible trade-offs between the nominal performance and the robustness. The span of the front is determined by the vectors $\boldsymbol{x}^p$ and $\boldsymbol{x}^r$. In this work, our goal is to identify a discrete subset of X_P, preferably distributed uniformly along the front. The proposed approach to accomplishing this aim has been described in Sections II.*B* through II.*D*. Figure 1 provides a conceptual illustration of the tolerance-aware multi-objective design problem formulation

B. Uncertainty Quantification Using Response Features

In this work, the robustness metric $F_r(\boldsymbol{x})$ is defined as the maximum level of input tolerances, measured using the variance σ of the zero-mean independent Gaussian probability distributions selected to characterize the statistical allocation of geometry parameter deviations. This is understood as the maximum σ for which the fabrication yield retains at 100 percent. The yield is defined as [47]

$$Y(\boldsymbol{x}) = \int_{X_f} p(\boldsymbol{y},\boldsymbol{x})d\boldsymbol{y} \quad (4)$$

where $p(\boldsymbol{y},\boldsymbol{x})$ is a joint probability density function describing statistical variations of the design $\boldsymbol{y}$ with respect to the evaluation parameter vector $\boldsymbol{x}$. The feasible space X_f contains

This article has been accepted for publication in a future issue of this journal, but has not been fully edited. Content may change prior to final publication. Citation information: DOI 10.1109/TAP.2022.3145462, IEEE Transactions on Antennas and Propagation

designs fulfilling the assumed performance specifications (here, those satisfying condition (1)). In practice, (4) can be approximately evaluated by means of Monte Carlo (MC) simulation as

$$Y(\boldsymbol{x}) = N_r^{-1} \sum_{k=1}^{N_r} H(\boldsymbol{x}^{(k)}) \tag{5}$$

where $\boldsymbol{x}^{(k)} = \boldsymbol{x} + d\boldsymbol{x}^{(k)}$, $k = 1, \ldots, N_r$, with deviation vectors $d\boldsymbol{x}^{(k)}$ generated according to the density function p. Reliable evaluation of (5) requires a large number of random samples, thus, it is an expensive process when realized directly using EM simulations. In practice, yield estimation if often accelerated using surrogate modeling techniques, e.g., [35]-[39].

Identification of $F_r(\boldsymbol{x}) = \sigma(\boldsymbol{x})$, the maximum input probability distribution variance ensuring 100-percent yield, is realized by solving

$$F_r(\boldsymbol{x}) = -\arg\max_{\sigma} \{Y(\boldsymbol{x}, \sigma) = 1\} \tag{6}$$

In (6), the explicit dependence of the yield on σ has been marked to emphasize the fact that this is the parameter determining the input tolerance levels, hence, the yield.

In this paper, to ensure computational efficiency, numerical evaluation of (6) is based on feature-based regression models as elaborated on below. The response feature technique has been originally proposed in [48] to improve reliability and to accelerate local tuning of antenna geometry parameters. The underlying concept is to reformulate the design problem using characteristic (or feature) points, e.g., frequency and level coordinates of resonances, or frequencies corresponding to specific levels of gain or axial ratio responses, extracted from the EM-simulated antenna outputs. The definition of the feature points is problem dependent so that information carried therein is sufficient to evaluate the system performance [48]. At the same time, focusing on characteristic points allows for reducing the complexity as well as nonlinearity, as the functional relationship between the feature point coordinates and geometry parameters is usually weakly nonlinear. As a result, it is possible to obtain expedited convergence of the optimization process [49], global search capabilities even when using local algorithms [50], or reduce the number of training data points for surrogate model construction [51].

Figure 2 shows the examples of input characteristics of a triple band antenna with the feature points defined to correspond to –10 dB levels of $|S_{11}|$. These points are sufficient to verify whether the operating bandwidths of the antenna adhere to given specifications (marked on the picture as thin lines). For other design situations, the required characteristic point setup might be different.

Following the performance specification setup of (1), the feature vector at the design $\boldsymbol{x}$, denoted as $\boldsymbol{P}(\boldsymbol{x})$ can be defined as

$$\begin{aligned} \boldsymbol{P}(\boldsymbol{x}) &= [p_1(\boldsymbol{x})\ p_2(\boldsymbol{x}) \ldots p_{2N}(\boldsymbol{x})]^T = \\ &= [f_1(\boldsymbol{x})\ f_2(\boldsymbol{x})\ \ldots\ f_{2N}(\boldsymbol{x})]^T \end{aligned} \tag{7}$$

where f_{2k-1} and f_{2k} are the frequencies corresponding to $P(\boldsymbol{x}, f_{2k-1}) = P(\boldsymbol{x}, f_{2k}) = P_{\max}$ for the kth operating band of the antenna, $k = 1, \ldots, N$. As mentioned before, these frequencies can be readily extracted from the EM-simulated antenna characteristics. Using $\boldsymbol{P}$, condition (1) can be rewritten as

$$p_{2k-1}(\boldsymbol{x}) \le f_{0.k} - B_k, \quad p_{2k}(\boldsymbol{x}) \ge f_{0.k} + B_k, \quad k = 1, \ldots, N \tag{8}$$

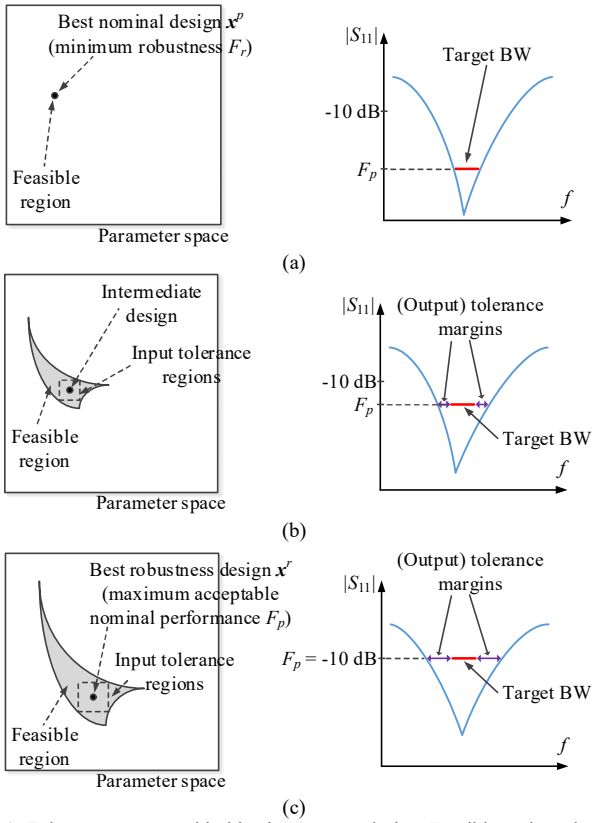

Fig. 1. Tolerance-aware multi-objective antenna design. Feasible region, shaded grey, contains designs satisfying performance requirements for a given value of F_p (note that the regions become larger with relaxing F_p). The right-hand-side plots illustrate exemplary antenna reflection responses versus target impedance bandwidth for different levels of target nominal performance threshold F_p: (a) for the best nominal design $\boldsymbol{x}^p$, assuming the uniqueness of solution to (2), the feasible region is a single-point set consisting of $\boldsymbol{x}^p$, therefore, the input tolerance level is zero; (b) for an intermediate design, the feasible region is larger and the most robust design is centred therein to maximize the input tolerance ranges ensuring performance requirements satisfaction; (c) for the best robustness design, corresponding the maximum acceptable level of F_p (e.g., –10 dB for antenna reflection), the input tolerance levels are the largest upon concluding the optimization process (cf. Section II.*C*). The family of designs obtained for different values of F_p form a Pareto set (performance vs. robustness trade-offs).

Due to a weakly-nonlinear relationship between the feature points and antenna geometry parameters, it is possible to set up a simple (e.g., linear) feature-based regression surrogates whose predictive power is sufficient to estimate the design robustness. Here, to represent $\boldsymbol{P}(\boldsymbol{x})$ in the vicinity of the current design, say $\boldsymbol{x}^{(i)}$, we use a linear model $\boldsymbol{L}_P^{(i)}(\boldsymbol{x})$, defined as

$$L_P^{(i)}(\boldsymbol{x}) = [p_{L.1}(\boldsymbol{x}) \ldots p_{L.2N}(\boldsymbol{x})]^T = \begin{bmatrix} l_{0.1} + \boldsymbol{L}_1^T(\boldsymbol{x} - \boldsymbol{x}^{(i)}) \\ \vdots \\ l_{0.2N} + \boldsymbol{L}_{2N}^T(\boldsymbol{x} - \boldsymbol{x}^{(i)}) \end{bmatrix} \tag{9}$$

The model coefficients are determined using $n + 1$ training points $\boldsymbol{x}_B^{(j)}$ and the corresponding feature vectors $\boldsymbol{P}(\boldsymbol{x}_B^{(j)})$, $j = 1, \ldots, n+1$, extracted from EM-simulated antenna characteristics at the respective points. The arrangement of training points is as follows: $\boldsymbol{x}_B^{(1)} = \boldsymbol{x}^{(i)}$, and $\boldsymbol{x}_B^{(j)} = \boldsymbol{x}^{(i)} + [0 \ldots 0\ d\ 0 \ldots 0]^T$ (d on the $(j-1)$th position). Here, we set $d = 3\sigma$, where σ is the variance of the Gaussian probability distribution assumed for parameter deviation.

The regression model can be identified analytically as

This article has been accepted for publication in a future issue of this journal, but has not been fully edited. Content may change prior to final publication. Citation information: DOI 10.1109/TAP.2022.3145462, IEEE Transactions on Antennas and Propagation

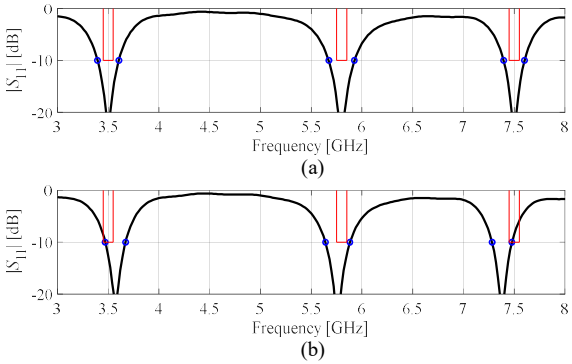

Fig. 2. Reflection characteristics of a triple-band antenna (—) and the response features corresponding to –10 dB $|S_{11}|$ levels (o). Exemplary exemplary design specifications shown using thin lines. The frequency coordinates of the feature points are sufficient to determine satisfaction/violation of performance requirements imposed on impedance matching, here for $P_{\max} = -10$ dB (cf. (1)): (a) design satisfying specifications, (b) design violating specifications.

$$\begin{bmatrix} l_{0.j} \\ \boldsymbol{L}_j \end{bmatrix} = \begin{bmatrix} 1 & (\boldsymbol{x}_B^{(1)} - \boldsymbol{x}^{(i)})^T \\ \vdots & \\ 1 & (\boldsymbol{x}_B^{(n+1)} - \boldsymbol{x}^{(i)})^T \end{bmatrix}^{-1} \begin{bmatrix} p_j(\boldsymbol{x}_B^{(1)}) \\ \vdots \\ p_j(\boldsymbol{x}_B^{(n+1)}) \end{bmatrix}, \quad j = 1, \ldots, 2N \quad (10)$$

The robustness-related objective $F_r(\boldsymbol{x})$ defined by (6) is computed through numerical integration of (4) using the regression surrogate (9). As mentioned before, performance condition (1) is equivalent to (8), which allows for estimating the yield $Y(\boldsymbol{x},\sigma)$ using a large number of random observables $\boldsymbol{x}_r^{(j)}$, which are allocated using the assumed probability distribution characterized by the variance σ.

The yield evaluation procedure works as follows:

1. Input parameter: variance σ;
2. Generate random observables $\{\boldsymbol{x}_r^{(j)}\}_{j=1,\ldots,Nr}$;
3. Evaluate regression surrogate $\boldsymbol{L}_P^{(i)}(\boldsymbol{x}_r^{(j)})$ for $j = 1, \ldots, N_r$;
4. Evaluate (8) for all observables using predicted feature points $p_{L.k}(\boldsymbol{x}_r^{(j)})$, $j = 1, \ldots, N_r$;
5. Estimate the yield $Y(\boldsymbol{x},\sigma)$ as in (5).

The function H in (5) is defined to be equal to one if (9) is satisfied, and zero otherwise. Using a large number of random samples allows for maintaining low yield estimation variance. To further accelerate the process, all steps in the above algorithm are vectorized (e.g., simultaneous evaluation of the regression model for all random samples is arranged as matrix multiplication due to the model being a linear function of its coefficients).

Now, evaluation of F_r is realized by solving (6) using a golden ratio search procedure [52] because having a common variance σ makes the problem a one-dimensional task. For other scenarios, e.g., probability distribution determined by multiple parameters (e.g., a given covariance matrix), other methods can be used such as gradient-based algorithms.

C. Iterative Rendition of Pareto-Optimal Designs

The tolerance-aware multi-objective optimization is carried out here as an iterative process leading to a discrete set of Pareto-optimal designs with respect to the performance and robustness objectives F_p and F_r, respectively, defined in Section II.*A*. The span of the Pareto front is determined by the best nominal design $\boldsymbol{x}^p$ (cf. (2)), and the most robust design $\boldsymbol{x}^r$, corresponding to the maximum acceptable target level $P_{\max}$ (e.g., –10 dB for input characteristics, or 3 dB for axial ratio responses). The aim is to generate N_P trade-off designs, with the first one being $\boldsymbol{x}^{(1)} = \boldsymbol{x}^p$. The value of the nominal objective function (2) at this design, denoted as $P_{\max.1}$, is

$$P_{\max.1} = \max\left\{ f \in \bigcup_{k=1}^{N} [f_{0k} - B_k, f_{0k} + B_k] : P(\boldsymbol{x}^p, f) \right\} \quad (11)$$

Let us set $P_{\max.NP} = P_{\max}$ (the maximum acceptable target level). The remaining $N_P - 1$ trade-off designs $\boldsymbol{x}^{(j)}$, $j = 2, \ldots, N_P$, will be generated for a sequence of target levels $P_{\max.j}$, $j = 1, \ldots, N_P$, allocated between $P_{\max.1}$ and $P_{\max.NP}$. In particular, equally-spaced distribution of the target levels

$$F_p(\boldsymbol{x}^{(j)}) = P_{\max.j} = P_{\max.1} + \left[P_{\max.N_P} - P_{\max.1} \right] \frac{j-1}{N_P - 1} \quad (12)$$

would result in equally-spaced Pareto set representation with respect to the nominal performance objective.

The design $\boldsymbol{x}^{(j)}$ is found by solving

$$\boldsymbol{x}^{(j)} = \arg\min_{\boldsymbol{x}} F_r(\boldsymbol{x}) \quad (13)$$

with $P_{\max}$ in (8) set to $P_{\max.j}$. In other words, the antenna is optimized for maximum robustness in the sense of (6), assuming that the target value therein is set to $P_{\max.j}$.

The problem (13) is solved iteratively following the trust-region (TR) principles [53]. At each iteration, a new approximation $\boldsymbol{x}^{(j.i+1)}$ of the design $\boldsymbol{x}^{(j)}$ is obtained as

$$\boldsymbol{x}^{(j.i+1)} = \arg\min_{\|\boldsymbol{x} - \boldsymbol{x}^{(j.i)}\| \le d^{(i)}} F_r(\boldsymbol{x}) \quad (14)$$

The starting point $\boldsymbol{x}^{(j.0)}$ is set to be $\boldsymbol{x}^{(j-1)}$. The evaluation process of $F_r(\boldsymbol{x})$ using feature-based surrogates has been described in detail in Section II.*B*. Note that the problem (14) is solved subject to a constraint $\|\boldsymbol{x} - \boldsymbol{x}^{(j.i)}\| \le d^{(i)}$; the trust region size $d^{(i)}$ is modified according to the typical TR rules [53]. Upon rendering a new point $\boldsymbol{x}^{(j.i+1)}$, the gain ratio is calculated as

$$r = \frac{F_r^{\#}(\boldsymbol{x}^{(j.i+1)}) - F_r(\boldsymbol{x}^{(j.i)})}{F_r(\boldsymbol{x}^{(j.i+1)}) - F_r(\boldsymbol{x}^{(j.i)})} \quad (15)$$

The denominator of r determines the improvement of the robustness as predicted by the feature-based regression model. The numerator is computed using $F_r^{\#}$, which is calculated in a similar manner as in Section II.*B*, but with the model $\boldsymbol{L}_P^{(j.i)}$ replaced by the linear model $\boldsymbol{L}_P^{\#(j.i)}$. The model $\boldsymbol{L}_P^{\#(j.i)}$ is constructed as in (9), (10) but with the coefficient vector $[l_{0.1} \ldots l_{0.2N}]^T$ replaced by $\boldsymbol{P}(\boldsymbol{x}^{(j.i+1)})$, the latter obtained from EM simulation results at $\boldsymbol{x}^{(j.i+1)}$. The reason for using $F_r^{\#}$ rather than an updated surrogate $\boldsymbol{L}_P^{(j.i+1)}$ is the computational efficiency: evaluation of the former requires only one EM analysis of the antenna at hand. The reliability of the assessment (15) is subject to the feature point gradients being relatively stable, i.e., not changing significantly between $\boldsymbol{x}^{(j.i)}$ and $\boldsymbol{x}^{(j.i+1)}$. This assumption normally holds because the distance between these two designs is comparable to σ, and—as mentioned before—the relationship between the feature point coordinates and antenna geometry parameters is weakly nonlinear.

The acceptance of the vector $\boldsymbol{x}^{(j.i+1)}$ is contingent upon r being positive. Otherwise, a new candidate design is obtained by repeating the iteration with a reduced size parameter $d^{(i)}$. The termination condition is based on the required resolution: we use the conditions $\|\boldsymbol{x}^{(i+1)} - \boldsymbol{x}^{(i)}\| < \varepsilon$ OR $d(i) < \varepsilon$, with $\varepsilon = 10^{-3}$. Figure 3 provides a graphical illustration of trade-off design generation using the concepts proposed in this paper.

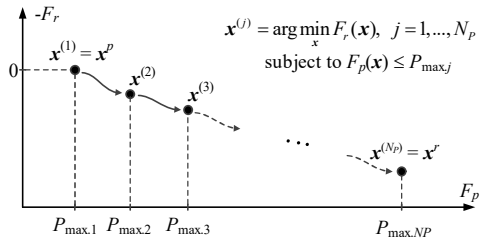

Fig. 3. Conceptual illustration of sequential generation of performance-robustness trade-off designs.

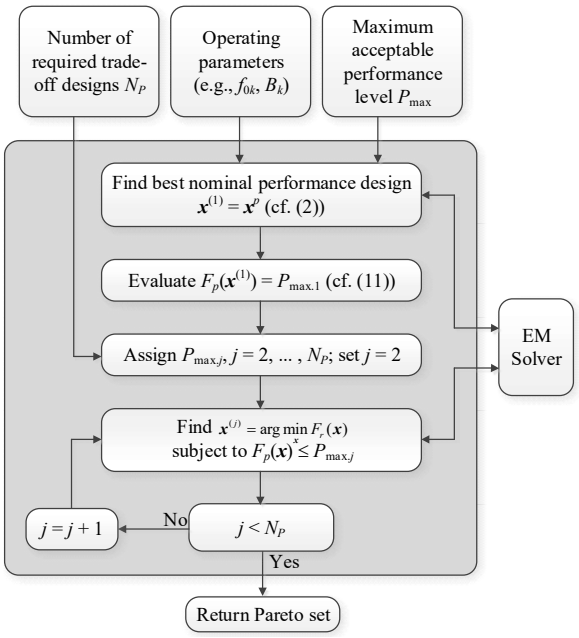

Fig. 4. Flow diagram of the proposed tolerance-aware multi-objective optimization algorithm using the feature-based regression surrogates and trust-region parameter adjustment process.

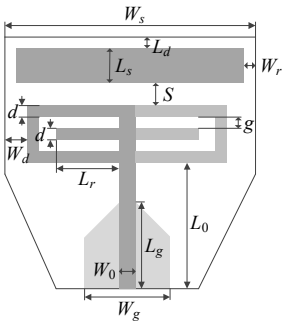

Fig. 5. Geometry of the dual-band dipole antenna with truncated substrate [54]. The light-gray shade marks the ground plane of the structure.

D. Optimization Procedure

Figure 4 shows the flow diagram of the proposed tolerance-aware multi-objective optimization procedure. Having determined the operating parameters and the maximum acceptable performance level $P_{\max}$, the best nominal design $\boldsymbol{x}^p$ is found, typically using local optimization. The performance objective value at this design $F_p(\boldsymbol{x}^p)$ is used, along with $P_{\max}$ and N_P, to determine the target performance levels $P_{\max,j}$. The performance-robustness trade-off designs are then obtained iteratively by solving the problem (13) with appropriate values of target performance levels.

III. Demonstration Examples

This section demonstrates the multi-objective design approach introduced in Section II using three examples of planar antennas, including two dual-band structures, and a quasi-Yagi antenna with an integrated balun. In all cases, the nominal performance function $F_p(\boldsymbol{x})$ is defined by the maximum in-band reflection level of the respective antenna, with an additional requirement imposed for the quasi-Yagi structure, and related to the minimum realized gain at the centre frequency. The robustness objective function $F_r(\boldsymbol{x})$ is defined as in (6), i.e., as the maximum variance of the probability distributions (describing the fabrication tolerances), for which 100-percent yield can still be achieved. For each structure, several trade-off designs are generated using the proposed methodology, and validated by means of EM-driven Monte Carlo simulations.

A. Example 1: Dual-Band Antenna with Truncated Substrate

The first verification example is a dual-band dipole antenna with truncated substrate [54] shown in Fig. 5. The structure is implemented on RO4003 substrate (ε_r = 3.38, h = 0.81 mm). The designable parameters are $\boldsymbol{x} = [L_{rr}\ d\ W_s\ W_d\ S\ L_d\ L_{gr}\ W_{gr}]^T$ (all dimensions are in millimeters except those ending with subscript r, which are relative). Other parameters are: W_r = 5 mm, L_s = 5 mm, L_0 = 25 mm, W_0 = 1.9 mm, $L_r = L_{rr}((W_s - W_0)/2 - W_d - d)$, $L_g = L_{gr}(L_0 - W_g/2 + W_0/2)$, $W_g = W_{gr}W_s$, and $g = W_d$. The computational model of the antenna is implemented in CST Microwave Studio and evaluated using the time-domain solver.

The target operating bandwidths of this antenna are given by f_{01} = 3.5 GHz, f_{02} = 4.2 GHz, and $B_1 = B_2$ = 80 MHz (cf. Section 2.1). Thus, we have 3.42 GHz to 3.58 GHz (lower band), and 4.12 GHz to 4.28 GHz (upper band). The best nominal performance design $\boldsymbol{x}^p$ = [0.91 1.45 48.01 3.66 1.80 4.97 1.00 0.38]^T corresponds to the maximum in-band reflection of $F_p(\boldsymbol{x}^p)$ = –15.1 dB. The robustness objective $F_r(\boldsymbol{x}^p)$ = 0 (cf. Section 2.1). Five more trade-off designs have been obtained, corresponding to $P_{\max.2}$ = –14 dB, $P_{\max.3}$ = –13 dB, through $P_{\max.6}$ = –10 dB (the highest acceptable in-band reflection level). Table I gathers numerical data concerning the performance-robustness trade-off designs, whereas Fig. 6 illustrates the corresponding Pareto set.

Furthermore, Fig. 7 provides visualization of the EM-driven Monte Carlo (MC) simulation for selected designs. The purpose of running MC was to verify whether the fabrication yield is indeed 100 percent for a given pair $\{F_p(\boldsymbol{x}^{(j)}), F_r(\boldsymbol{x}^{(j)})\}$. According to the obtained results, it is typically between 98 and 100 percent (design dependent). However, it should be emphasized that MC was executed using only 500 samples (to avoid excessive CPU expenses), therefore, the standard deviation of yield estimation is relatively high.

It should also be mentioned that the proposed methodology is computationally efficient. The average cost of rendering one trade-off design is only about 62 EM simulations of the antenna structure. The primary acceleration factor is the incorporation of feature-based surrogates as described in Section II.*B*.

This article has been accepted for publication in a future issue of this journal, but has not been fully edited. Content may change prior to final publication. Citation information: DOI 10.1109/TAP.2022.3145462, IEEE Transactions on Antennas and Propagation

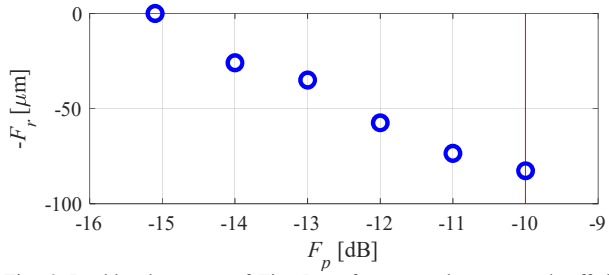

Fig. 6. Dual-band antenna of Fig. 5: performance-robustness trade-off designs obtained using the proposed procedure for multi-objective optimization with tolerances. The vertical line marks the maximum acceptable in-band reflection level.

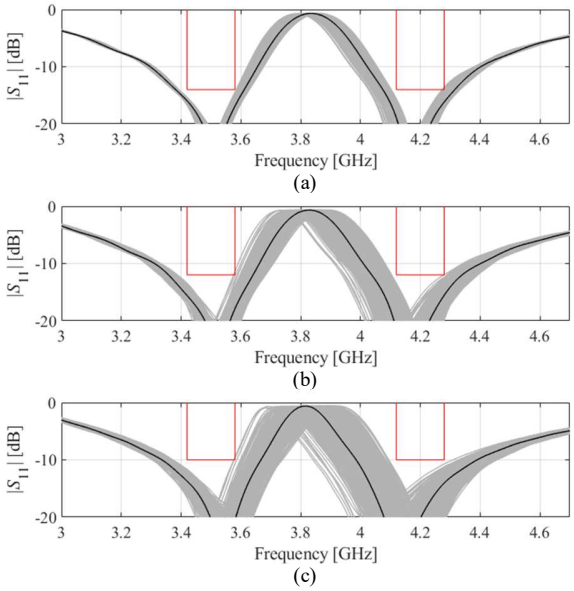

Fig. 7. EM-driven Monte Carlo simulation for selected trade-off designs of Table I. Black line shows the antenna response at the given trade-off design: (a) design $\boldsymbol{x}^{(2)}$, (b) design $\boldsymbol{x}^{(4)}$, (c) design $\boldsymbol{x}^{(6)}$, grey lines correspond to 500 random observables generated according to the assumed probability distribution with the variance equal to F_r. Thin lines denote design specifications.

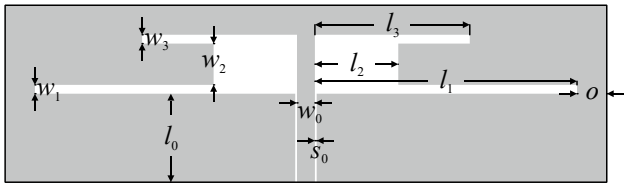

Fig. 8. Geometry of the dual-band uniplanar dipole antenna with coplanar waveguide feed [55].

B. Example 2: Dual-Band Uniplanar Dipole Antenna

Our second example is a dual-band uniplanar dipole antenna with coplanar waveguide feed [55] shown in Fig. 8. The structure is implemented on RF-35 substrate (ε_r = 3.5, h = 0.76 mm). The designable parameters are $\boldsymbol{x} = [l_1\ l_2\ l_3\ w_1\ w_2\ w_3]^T$ (dimensions mm). Other parameters are l_0 = 30 mm, w_0 = 3 mm, s_0 = 0.15 mm, and o = 5 mm. The computational model of the antenna is implemented in CST Microwave Studio and evaluated using its time-domain solver.

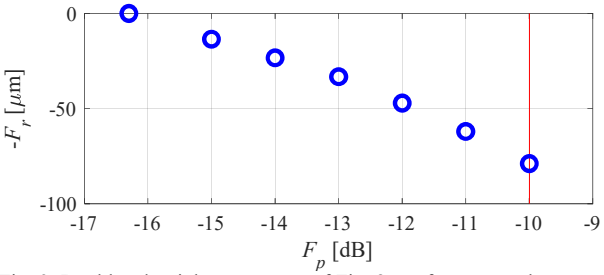

Fig. 9. Dual-band uniplanar antenna of Fig. 8: performance-robustness trade-off designs obtained using the proposed procedure for multi-objective optimization with tolerances. The vertical line marks the maximum acceptable in-band reflection level.

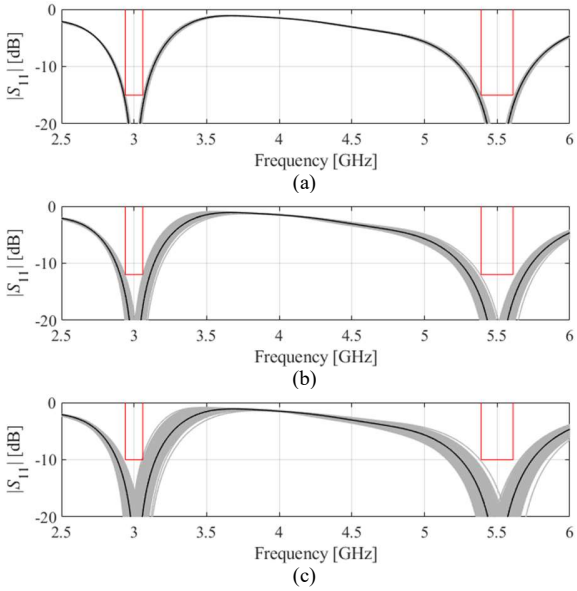

Fig. 10. EM-driven Monte Carlo simulation for selected trade-off designs of Table I. Black line shows the antenna response at the given trade-off design: (a) design $\boldsymbol{x}^{(2)}$, (b) design $\boldsymbol{x}^{(5)}$, (c) design $\boldsymbol{x}^{(7)}$, grey lines correspond to 500 random observables generated according to the assumed probability distribution with the variance equal to F_r. Thin lines denote design specifications.

The target operating bandwidths of this antenna are given by f_{01} = 3.0 GHz, f_{02} = 5.5 GHz, B_1 = 60 MHz, and B_2 = 110 MHz (cf. Section II.*A*). Thus, we have 2.94 GHz to 3.06 GHz (lower band), and 5.39 GHz to 5.61 GHz (upper band). The best nominal performance design $\boldsymbol{x}^p$ = [30.37 11.51 19.28 0.41 2.31 1.21]^T corresponds to the maximum in-band reflection of $F_p(\boldsymbol{x}^p)$ = –16.3 dB. For this structure, six additional trade-off designs have been generated, corresponding to $P_{\max.2}$ = –15 dB, $P_{\max.3}$ = –14 dB, through $P_{\max.7}$ = –10 dB (the highest acceptable in-band reflection level). The numerical data and visualization of the Pareto set are provided in Table II and Fig. 9, respectively. Visualization of the EM-based Monte Carlo simulation for selected trade-off designs has been shown in Fig. 10. Similarly as for the first example, the estimated yield is close to 100 percent for all Pareto-optimal vectors $\boldsymbol{x}^{(j)}$, which corroborates a good predictive power of the response feature surrogates. The average computational cost of generating the trade-off designs is only about 40 EM antenna analyses per point.

This article has been accepted for publication in a future issue of this journal, but has not been fully edited. Content may change prior to final publication. Citation information: DOI 10.1109/TAP.2022.3145462, IEEE Transactions on Antennas and Propagation

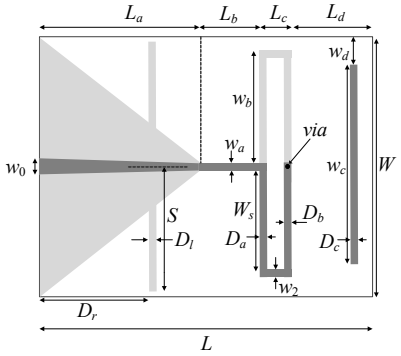

Fig. 11. Geometry of quasi-Yagi antenna with integrated balun [53]. Light-gray shade indicates ground-plane metallization.

TABLE I DUAL-BAND ANTENNA OF FIG. 5: RESULTS OF MULTI-OBJECTIVE DESIGN WITH TOLERANCES

Design	Objectives		Geometry parameters [absolute in mm, relative unitless]							
	F_p [dB]	F_r [μm]	L_{rr}	d	W_s	W_d	S	L_d	L_{gr}	W_{gr}
$\boldsymbol{x}^{(1)} = \boldsymbol{x}^r$	–15.1	0	0.91	1.45	48.01	3.66	1.80	4.97	1.00	0.38
$\boldsymbol{x}^{(2)}$	–14	25.9	0.92	1.42	47.99	3.62	1.78	4.93	1.00	0.38
$\boldsymbol{x}^{(3)}$	–13	35.0	0.92	1.40	47.99	3.65	1.80	4.95	1.00	0.38
$\boldsymbol{x}^{(4)}$	–12	57.5	0.92	1.34	47.98	3.72	2.01	4.68	0.99	0.39
$\boldsymbol{x}^{(5)}$	–11	73.5	0.92	1.24	47.87	3.65	2.32	4.58	0.99	0.38
$\boldsymbol{x}^{(6)} = \boldsymbol{x}^r$	–10	82.7	0.92	1.20	47.85	3.68	2.39	4.62	0.99	0.38

TABLE II DUAL-BAND UNIPLANAR ANTENNA OF FIG. 8: RESULTS OF MULTI-OBJECTIVE DESIGN WITH TOLERANCES

Design	Objectives		Geometry parameters [mm]					
	F_p [dB]	F_r [μm]	l_1	l_2	l_3	w_1	w_2	w_3
$\boldsymbol{x}^{(1)} = \boldsymbol{x}^r$	–16.3	0	30.37	11.51	19.28	0.41	2.31	1.21
$\boldsymbol{x}^{(2)}$	–15	13.5	30.31	11.52	19.28	0.38	2.32	1.21
$\boldsymbol{x}^{(3)}$	–14	23.3	30.30	11.51	19.28	0.38	2.32	1.21
$\boldsymbol{x}^{(4)}$	–13	33.2	30.29	11.51	19.27	0.38	2.31	1.21
$\boldsymbol{x}^{(5)}$	–12	47.1	30.27	11.51	19.29	0.37	2.28	1.20
$\boldsymbol{x}^{(6)}$	–12	62.0	30.25	11.51	19.29	0.38	2.27	1.20
$\boldsymbol{x}^{(7)} = \boldsymbol{x}^r$	–10	78.9	30.23	11.52	19.31	0.38	2.26	1.19

C. Example 3: Quasi-Yagi Antenna with Integrated Balun

Our last example is a quasi-Yagi antenna with integrated balun [56] shown in Fig. 11. The antenna is implemented on RO4003 substrate (ε_r = 3.38, h = 1.5 mm). The independent design parameters are $\boldsymbol{x} = [L_a\ L_b\ L_c\ L_d\ W\ w_a\ D_a\ D_b\ D_c\ D_{lr}\ D_{rr}\ S_r\ w_{br}\ w_{cr}]^T$. The parameters with subscript r are relative. We have $D_l = D_{lr}L_a$, $D_r = D_{rr}L_a$, $S = S_rW$, $w_b = w_{br}W/2$, $w_c = w_{cr}W$, w_0 = 3.4 mm. The unit for the absolute dimensions is mm. The computational model of the antenna is implemented and simulated in CST Microwave Studio.

The target operating bandwidth is given by f_{01} = 2.5 GHz and B_1 = 50 MHz (cf. Section II.*A*). Thus, the bandwidth is 2.45 GHz to 2.55 GHz. An additional condition is that the realized gain at 2.5 GHz is to be at least 7.9 (i.e., 8 dB with the tolerance of 0.1 dB). The best nominal performance design $\boldsymbol{x}^p$ = [20.21 12.33 16.47 26.09 52.06 1.83 1.02 4.39 4.26 0.37 0.44 0.98 0.71 0.72]^T corresponds to the maximum in-band reflection of $F_p(\boldsymbol{x}^p)$ = –17.0 dB. In this case, seven additional trade-off designs have been generated, corresponding to $P_{\max.2}$ = –16 dB, $P_{\max.3}$ = –15 dB, through $P_{\max.7}$ = –10 dB (the highest acceptable in-band reflection level).

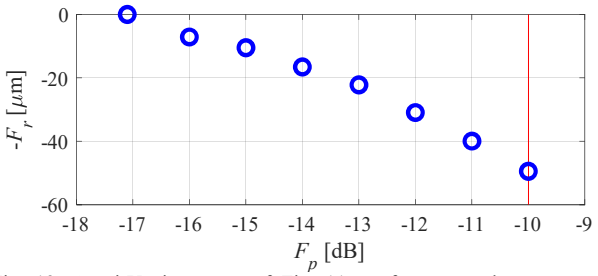

Fig. 12. Quasi-Yagi antenna of Fig. 11: performance-robustness trade-off designs obtained using the proposed procedure for multi-objective optimization with tolerances. The vertical line marks the maximum acceptable in-band reflection level.

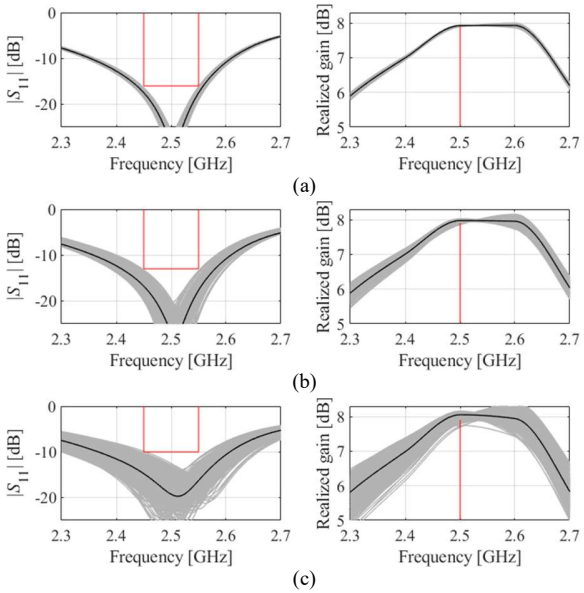

Fig. 13. EM-driven Monte Carlo simulation for selected trade-off designs of Table I. Black line shows the antenna response at the given trade-off design: (a) design $\boldsymbol{x}^{(2)}$, (b) design $\boldsymbol{x}^{(5)}$, (c) design $\boldsymbol{x}^{(8)}$, grey lines correspond to 500 random observables generated according to the assumed probability distribution with the variance equal to F_r. Thin lines denote design specifications.

The numerical data and visualization of the Pareto set are provided in Table III and Fig. 12, respectively. Visualization of the EM-based Monte Carlo simulation for selected trade-off designs has been shown in Fig. 13. Also for this antenna, the estimated yield is close to 100 percent for all vectors $\boldsymbol{x}^{(j)}$, although the differences between the perfect and actual yield are more significant: the average estimated yield is 97 percent but the values obtained for the last design $\boldsymbol{x}^{(8)}$ is 90 percent, which is due to two factors: (i) higher dimensionality of the parameter space (fourteen parameters versus eight and six for the first two examples), and (ii) limited prediction power of the surrogate model for larger values of input tolerances. At the same time, one needs to remember that MC based on only 500 samples is not perfectly reliable.

The average computational cost of obtaining the trade-off designs is about 82 EM antenna simulations per point, which is slightly higher than for the previous examples; however, it can be observed that the cost scales close-to-linearly as shown in Fig. 14. This property is a consequence of using linear regression surrogate, the setup cost of which is proportional to the number of antenna parameters.

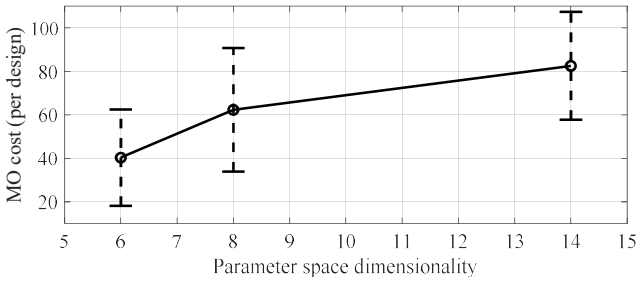

Fig. 14. Computational cost of MO with tolerances versus parameter space dimensionality. The data gathered from examples presented in Sections III.*A* through III.*C* (antenna of Fig. 8 – six parameters, antenna of Fig. 5 – eight parameters, antenna of Fig. 11 – fourteen parameters). The vertical bars represent standard deviation of the cost, calculated for the trade-off design set.

TABLE III QUASI-YAGI ANTENNA OF FIG. 11: RESULTS OF MULTI-OBJECTIVE DESIGN WITH TOLERANCES

Design	Objectives		Geometry parameters [absolute in mm, relative unitless]												
	F_p [dB]	F_r [μm]	L_a	L_b	L_c	L_d	W	w_a	D_a	D_b	D_c	D_{lr}	D_{rr}	S_r	w_{br}	D_a
1	–17	0	20.2	12.3	16.5	26.1	52.1	1.83	1.02	4.39	4.26	0.37	0.44	0.98	0.71	0.72
2	–16	7.1	20.2	12.3	16.5	26.0	52.1	1.73	1.02	4.34	4.15	0.38	0.44	0.98	0.71	0.72
3	–15	10.5	20.3	12.4	16.5	26.0	52.1	1.73	1.03	4.34	4.11	0.38	0.43	0.98	0.71	0.72
4	–14	16.6	20.2	12.4	16.5	26.0	52.1	1.64	1.02	4.36	4.04	0.38	0.40	0.99	0.71	0.72
5	–13	22.2	20.2	12.4	16.5	26.0	52.1	1.69	1.02	4.41	4.02	0.38	0.40	0.99	0.71	0.73
6	–12	30.9	20.3	12.4	16.5	26.0	52.1	1.66	1.01	4.48	4.06	0.37	0.40	0.98	0.71	0.73
7	–11	39.9	20.5	12.4	16.4	26.1	52.1	1.49	1.01	4.50	3.99	0.38	0.40	0.98	0.71	0.73
8	–10	49.5	20.6	12.5	16.3	26.1	52.1	1.45	1.01	4.50	3.98	0.35	0.40	0.97	0.71	0.73

IV. CONCLUSION

This paper proposed a novel technique for multi-objective optimization of antenna structures with tolerances. The aim is to produce a family of designs representing the best possible trade-offs between the nominal performance (i.e., without accounting for manufacturing tolerances), and the robustness. The latter is quantified as the maximum levels of input tolerances for which the perfect (100-percent) yield is still possible. The key components of the presented approach are response feature surrogates, the employment of which contributes to both the reliability of the optimization process and its computational efficiency. Furthermore, embedding the search process into the trust-region framework ensures convergence while allowing us to reduce the computational cost even further. Comprehensive validation carried out using three microstrip antennas indicates that the presented methodology permits expedited and accurate rendition of performance-robustness trade-off designs. The CPU expenses vary from forty to about eighty EM antenna simulations per design, for structures described by six to fourteen parameters. The reliability of the algorithm was validated through EM-driven Monte Carlo simulation at the selected Pareto-optimal points. The optimization framework introduced in this work may be useful for determining the required accuracy of the fabrication process as well as for comparing alternative antenna structures with respect to their tolerance immunity.

ACKNOWLEDGMENT

The authors would like to thank Dassault Systemes, France, for making CST Microwave Studio available.

REFERENCES

[1] J.E. Rayas-Sanchez, S. Koziel, and J.W. Bandler, "Advanced RF and microwave design optimization: a journey and a vision of future trends," *IEEE J. Microwaves*, vol. 1, no. 1, pp. 481-493, 2021.

[2] A. K. Prasad and S. Roy, "Reduced dimensional Chebyshev-polynomial chaos approach for fast mixed epistemic-aleatory uncertainty quantification of transmission line networks," *IEEE Trans. Comp. Packaging Manufacturing Techn.*, vol. 9, no. 6, pp. 1119-1132, 2019.

[3] Y. Li, Y. Ding, and E. Zio, "Random fuzzy extension of the universal generating function approach for the reliability assessment of multi-state systems under aleatory and epistemic uncertainties," *IEEE Trans. Reliability*, vol. 63, no. 1, pp. 13-25, 2014.

[4] B. B. Q. Elias, P. J. Soh, A. A. Al-Hadi, and P. Akkaraekthalin, "Gain optimization of low-profile textile antennas using CMA and active mode subtraction method," *IEEE Access*, vol. 9, pp. 23691-23704, 2021.

[5] Z. Zhang, H. Chen, F. Jiang, Y. Yu, and Q. S. Cheng, "A benchmark test suite for antenna S-parameter optimization," *IEEE Trans. Ant. Propag.*, early access, 2021.

[6] Y. -X. Zhang, Y. -C. Jiao, and L. Zhang, "Antenna array directivity maximization with sidelobe level constraints using convex optimization," *IEEE Trans. Ant. Propag.*, vol. 69, no. 4, pp. 2041-2052, 2021.

[7] S. Koziel and A. Pietrenko-Dabrowska, "Robust parameter tuning of antenna structures by means of design specification adaptation," *IEEE Trans. Ant. Propag.*, Early access, 2021.

[8] S. Kojima, T. Mitani, and N. Shinohara, "Array optimization for maximum beam collection efficiency to an arbitrary receiving plane in the near field," *IEEE Open J. Ant. Propag.*, vol. 2, pp. 95-103, 2021.

[9] A. D. Boursianis, M. S. Papadopoulou, J. Pierezan, V. C. Mariani, L. S. Coelho, P. Sarigiannidis, S. Koulouridis, and S. K. Goudos, "Multiband patch antenna design using nature-inspired optimization method," *IEEE Open J. Ant. Propag.*, vol. 2, pp. 151-162, 2021.

[10] Q. Xu, S. Zeng, F. Zhao, R. Jiao, and C. Li, "On formulating and designing antenna arrays by evolutionary algorithms," *IEEE Trans. Ant. Propag.*, vol. 69, no. 2, pp. 1118-1129, 2021.

[11] A. A. Al-Azza, A. A. Al-Jodah, and F. J. Harackiewicz, "Spider monkey optimization: a novel technique for antenna optimization," *IEEE Antennas Wireless Propag. Lett.*, vol. 15, pp. 1016-1019, 2016.

[12] A. Darvish and A. Ebrahimzadeh, "Improved fruit-fly optimization algorithm and its applications in antenna arrays synthesis," *IEEE Trans. Antennas Propag.*, vol. 66, no. 4, pp. 1756-1766, 2018.

[13] T. C. Bora, L. Lebensztajn, and L. D. S. Coelho, „Non-dominated sorting genetic algorithm based on reinforcement learning to optimization of broad-band reflector antennas satellite," *IEEE Trans. Magn.*, vol. 48, no. 2, pp. 767-770, 2012.

[14] Z. Bayraktar, M. Komurcu, J. A. Bossard, and D. H. Werner, "The wind driven optimization technique and its application in electromagnetics," *IEEE Trans. Antennas Propag.*, vol. 61, no. 5, pp. 2745-2757, 2013.

[15] Y. Zhao, C. Sun, J. Zeng, Y. Tan, G. Zhang, "A surrogate-ensemble assisted expensive many-objective optimization," *Knowledge-Based Syst.*, vol. 211, art. no. 106520, 2021.

[16] S. Koziel and A. T. Sigurdsson, "Multi-fidelity EM simulations and constrained surrogate modeling for low-cost multi-objective design optimization of antennas," *IET Microwaves Ant. Prop.*, vol. 12, no. 13, pp. 2025-2029, 2018.

[17] S. Xiao, G. Q. Liu, K. L. Zhang, Y. Z. Jing, J. H. Duan, P. Di Barba, and J. K. Sykulski, "Multi-objective Pareto optimization of electromagnetic devices exploiting kriging with Lipschitzian optimized expected improvement," *IEEE Trans. Magn.*, vol. 54, no. 3, art. no. 7001704, 2018.

[18] D. I. L. de Villiers, I. Couckuyt, and T. Dhaene, "Multi-objective optimization of reflector antennas using kriging and probability of improvement," *Int. Symp. Ant. Prop.*, pp. 985-986, San Diego, USA, 2017.

[19] J. P. Jacobs, "Characterization by Gaussian processes of finite substrate size effects on gain patterns of microstrip antennas," *IET Microwaves Ant. Prop.*, vol. 10, no. 11, pp. 1189-1195, 2016.

[20] Z. Lv, L. Wang, Z. Han, J. Zhao, and W. Wang, "Surrogate-assisted particle swarm optimization algorithm with Pareto active learning for expensive multi-objective optimization," *IEEE J. Automatica Sinica*, vol. 6, no. 3, pp. 838-849, 2019.

[21] S. Koziel and A. Pietrenko-Dabrowska, "Rapid multi-objective optimization of antennas using nested kriging surrogates and single-

fidelity EM simulation models," *Eng. Comp.*, vol. 37, no. 4, pp. 1491-1512, 2019.

[22] S. Koziel and A. Pietrenko-Dabrowska, "Fast multi-objective optimization of antenna structures by means of data-driven surrogates and dimensionality reduction," *IEEE Access*, vol. 8, pp. 183300-183311, 2020.

[23] S. Koziel and S. Ogurtsov, "Multi-objective design of antennas using variable-fidelity simulations and surrogate models," *IEEE Trans. Antennas Prop.*, vol. 61, no. 12, pp. 5931-5939, 2013.

[24] Y. Liu, Q. S. Cheng, and S. Koziel, "A generalized SDP multi-objective optimization method for EM-based microwave device design," *Sensors*, vol. 19, no. 14, 2019.

[25] S. D. Unnsteinsson and S. Koziel, "Generalized Pareto ranking bisection for computationally feasible multi-objective antenna optimization," *Int. J. RF & Microwave CAE*, vol. 28, no. 8, art. no. e21406, 2018.

[26] A. Toktas, D. Ustun, and M. Tekbas, "Multi-objective design of multi-layer radar absorber using surrogate-based optimization," *IEEE Trans. Microw. Theory Techn*., vol. 67, no. 8, pp. 3318-3329, Aug. 2019.

[27] N. Taran, D. M. Ionel, and D. G. Dorrell, "Two-level surrogate-assisted differential evolution multi-objective optimization of electric machines using 3-D FEA," *IEEE Trans. Magn.*, vol. 54, no. 11, art. no. 8107605, 2018.

[28] S. Koziel and S. Ogurtsov, "Multi-objective design of antennas using variable-fidelity simulations and surrogate models," *IEEE Trans. Antennas Prop.*, vol. 61, no. 12, pp. 5931-5939, 2013.

[29] M. Rossi, A. Dierck, H. Rogier, and D. Vande Ginste, "A stochastic framework for the variability analysis of textile antennas," *IEEE Trans. Ant. Prop.*, vol. 62, no. 16, pp. 6510-6514, 2014.

[30] J. Du and C. Roblin, "Stochastic surrogate models of deformable antennas based on vector spherical harmonics and polynomial chaos expansions: application to textile antennas," *IEEE Trans. Ant. Propag.*, vol. 66, no. 7, pp. 3610-3622, 2018.

[31] J. E. Rayas-Sanchez and V. Gutierrez-Ayala, "EM-based statistical analysis and yield estimation using linear-input and neural-output space mapping," *IEEE MTT-S Int. Microwave Symp. Digest (IMS)*, pp. 1597-1600, 2006.

[32] J. Zhang, C. Zhang, F. Feng, W. Zhang, J. Ma, and Q. J. Zhang, "Polynomial chaos-based approach to yield-driven EM optimization," *IEEE Trans. Microwave Theory Tech.*, vol. 66, no. 7, pp. 3186-3199, 2018.

[33] J. S. Ochoa and A. C. Cangellaris, "Random-space dimensionality reduction for expedient yield estimation of passive microwave structures," *IEEE Trans. Microwave Theory Techn.*, vol. 61, no. 12, pp. 4313-4321, 2013.

[34] Q. Wu, W. Chen, C. Yu, H. Wang, and W. Hong, "Multilayer machine learning-assisted optimization-based robust design and its applications to antennas and arrays," *IEEE Trans. Ant. Prop.*, Early view, 2021.

[35] H. L. Abdel-Malek, A. S. O. Hassan, E. A. Soliman, and S. A. Dakroury, "The ellipsoidal technique for design centering of microwave circuits exploiting space-mapping interpolating surrogates," *IEEE Trans. Microwave Theory Techn.*, vol. 54, no. 10, pp. 3731-3738, 2006.

[36] B. Ma, G. Lei, C. Liu, J. Zhu, and Y. Guo, „Robust tolerance design optimization of a PM claw pole motor with soft magnetic composite cores," *IEEE Trans. Magn.*, vol. 54, no. 3, art. no. 8102404, 2018.

[37] Z. Ren, S. He, D. Zhang, Y. Zhang, and C. S. Koh, "A possibility-based robust optimal design algorithm in preliminary design state of electromagnetic devices," *IEEE Trans. Magn.*, vol. 52, no. 3, art. no. 7001504, 2016.

[38] D. Spina, F. Ferranti, G. Antonini, T. Dhaene, and L. Knockaert, "Efficient variability analysis of electromagnetic systems via polynomial chaos and model order reduction," *IEEE Trans. Comp. Packaging Manufacturing Techn.*, vol. 4, no. 6, pp. 1038-1051, 2014.

[39] H. Acikgoz and R. Mittra, "Stochastic polynomial chaos expansion analysis of a split-ring resonator at terahertz frequencies," *IEEE Trans. Ant. Propag.*, vol. 66, no. 4, pp. 2131-2134, 2018.

[40] L. Leifsson, X. Du, and S. Koziel, „Efficient yield estimation of multiband patch antennas by polynomial chaos-based Kriging," *Int. J. Numer. Model.*, vol. 33, no. 6, Art. no. e2722, 2020.

[41] A. Pietrenko-Dabrowska, S. Koziel, and M. Al-Hasan, „Expedited yield optimization of narrow- and multi-band antennas using performance-driven surrogates," *IEEE Access*, vol. 8, pp. 143104-143113, 2020.

[42] B. Xia, Z. Ren, and C. -S. Koh, "Utilizing Kriging surrogate models for multi-objective robust optimization of electromagnetic devices," *IEEE Trans. Magn.*, vol. 50, no. 2, art. no. 7017104, 2014.

[43] B. Liu, H. Aliakbarian, Z. Ma, G. A. Vandenbosch, G. Gielen, and P. Excell, "An efficient method for antenna design optimization based on evolutionary computation and machine learning techniques," *IEEE Trans. Antennas Propag.*, vol. 62, pp. 7-18, 2014.

[44] J. A. Easum, J. Nagar, P. L. Werner, and D. H. Werner, "Efficient multi-objective antenna optimization with tolerance analysis through the use of surrogate models," *IEEE Trans. Ant. Prop.*, vol. 66, no. 12, pp. 6706-6715, 2018.

[45] K. Deb, A. Pratap, S. Agarwal, and T. Meyarivan, "A fast and elitist multiobjective genetic algorithm: NSGA-II," *IEEE Trans. Evol. Comput.*, vol. 6, pp. 182-197, Apr. 2002.

[46] K. Deb, *Multi-Objective Optimization Using Evolutionary Algorithms.* Wiley, New York, 2001.

[47] A. S. O. Hassan, H. L. Abdel-Malek, A. S. A. Mohamed, T. M. Abuelfadl, and A. E. Elqenawy, "Statistical design centering of RF cavity linear accelerator via non-derivative trust region optimization," *IEEE Int. Conf. Numerical EM Multiphysics Modeling Opt. (NEMO)*, pp. 1-3, 2015.

[48] S. Koziel, "Fast simulation-driven antenna design using response-feature surrogates," *Int. J. RF & Microwave CAE*, vol. 25, no. 5, pp. 394-402, 2015.

[49] A. Pietrenko-Dabrowska and S. Koziel, „Fast design closure of compact microwave components by means of feature-based metamodels," *Electronics*, vol. 10, no. 1, art. no. 10, 2021.

[50] S. Koziel and A. Pietrenko-Dabrowska, "Expedited feature-based quasi-global optimization of multi-band antennas with Jacobian variability tracking," *IEEE Access*, vol. 8, pp. 83907-83915, 2020.

[51] A. Pietrenko-Dabrowska and S. Koziel, "Simulation-driven antenna modeling by means of response features and confined domains of reduced dimensionality," *IEEE Access*, vol. 8, pp. 228942-228954, 2020.

[52] W. H. Press, S. A. Teukolsky, W. T. Vetterling, and B. P. Flannery, "Golden section search in one dimension," in *Numerical Recipes: The Art of Scientific Computing* (3rd ed.), Cambridge University Press, New York, 2007.

[53] A. R. Conn, N. I. M. Gould, and P. L. Toint, *Trust Region Methods*, MPS-SIAM Series on Optimization, 2000.

[54] M. Qudrat-E-Maula, and L. Shafai, "A dual band microstrip dipole antenna," *Int. Symp. Ant. Technology and Applied Electr. (ANTEM)*, pp. 1-2, Victoria, BC, Canada, July 13-16, 2014.

[55] Y. -C. Chen, S. -Y. Chen, and P. Hsu, "Dual-band slot dipole antenna fed by a coplanar waveguide," *IEEE Int. Symp. Ant. Prop.*, pp. 3589-3592, 2006.

[56] M. Farran, S. Boscolo, A. Locatelli, A.D. Capobianco, M. Mirio, V. Ferrari, and D. Modotto, "Compact quasi-Yagi antenna with folded dipole fed by tapered integrated balun," *Electronics Letters*, vol. 52, no. 10, pp. 789-790, 2016.

SLAWOMIR KOZIEL received the M.Sc. and Ph.D. degrees in electronic engineering from Gdansk University of Technology, Poland, in 1995 and 2000, respectively. He also received the M.Sc. degrees in theoretical physics and in mathematics, in 2000 and 2002, respectively, as well as the PhD in mathematics in 2003, from the University of Gdansk, Poland. He is currently a Professor with the Department of Engineering, Reykjavik University, Iceland. His research interests include CAD and modeling of microwave and antenna structures, simulation-driven design, surrogate-based optimization, space mapping, circuit theory, analog signal processing, evolutionary computation and numerical analysis.

ANNA PIETRENKO-DABROWSKA received the M.Sc. and Ph.D. degrees in electronic engineering from Gdansk University of Technology, Poland, in 1998 and 2007, respectively. Currently, she is an Associate Professor with Gdansk University of Technology, Poland. Her research interests include simulation-driven design, design optimization, control theory, modeling of microwave and antenna structures, numerical analysis.